

## Noninvasive Targeted Transcranial Neuromodulation via Focused Ultrasound Gated Drug Release from Nanoemulsions

Raag D. Airan,<sup>\*,†,‡,§,||</sup> Randall A. Meyer,<sup>‡,||</sup> Nicholas P. K. Ellens,<sup>†</sup> Kelly R. Rhodes,<sup>‡</sup> Keyvan Farahani,<sup>†,⊥</sup> Martin G. Pomper,<sup>‡,||,¶</sup> Shilpa D. Kadam,<sup>∇,○</sup> and Jordan J. Green<sup>\*,‡,||,#,◆</sup>

<sup>†</sup>Department of Radiology and Radiological Science, Johns Hopkins University School of Medicine, Baltimore, Maryland 21231, United States

<sup>‡</sup>Department of Biomedical Engineering and the Translational Tissue Engineering Center, Johns Hopkins University School of Medicine, Baltimore, Maryland 21231, United States

<sup>§</sup>Department of Radiology, Stanford University, Stanford, California 94305, United States

<sup>||</sup>Institute for NanoBioTechnology, Johns Hopkins University, Baltimore, Maryland 21231, United States

<sup>⊥</sup>National Cancer Institute/National Institutes of Health, Bethesda, Maryland 20892, United States

<sup>#</sup>Department of Oncology, Johns Hopkins University School of Medicine, Baltimore, Maryland 21231, United States

<sup>∇</sup>Neuroscience Laboratory, Hugo Moser Research Institute, Kennedy Krieger Institute, Baltimore, Maryland 21287, United States

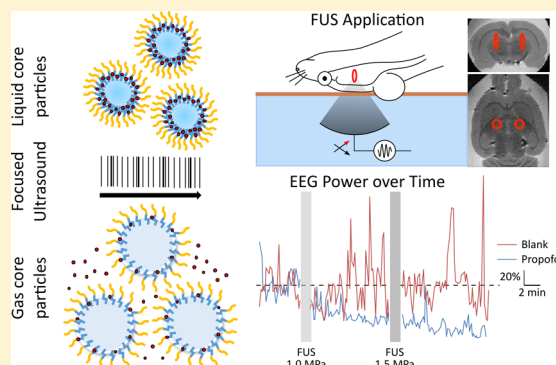
<sup>○</sup>Department of Neurology, Johns Hopkins Medical Institutions, Baltimore, Maryland 21287, United States

<sup>◆</sup>Departments of Neurosurgery, Ophthalmology, and Materials Science and Engineering, Johns Hopkins University School of Medicine, Baltimore, Maryland 21231, United States

### Supporting Information

**ABSTRACT:** Targeted, noninvasive neuromodulation of the brain of an otherwise awake subject could revolutionize both basic and clinical neuroscience. Toward this goal, we have developed nanoparticles that allow noninvasive uncaging of a neuromodulatory drug, in this case the small molecule anesthetic propofol, upon the application of focused ultrasound. These nanoparticles are composed of biodegradable and biocompatible constituents and are activated using sonication parameters that are readily achievable by current clinical transcranial focused ultrasound systems. These particles are potent enough that their activation can silence seizures in an acute rat seizure model. Notably, there is no evidence of brain parenchymal damage or blood-brain barrier opening with their use. Further development of these particles promises noninvasive, focal, and image-guided clinical neuromodulation along a variety of pharmacological axes.

**KEYWORDS:** Neuromodulation, focused ultrasound, nanoparticles, gated drug release



A long sought after goal of both clinical and basic neuroscience is the ability to focally modulate the activity of a spatially delimited region of the brain, noninvasively, and in a safe and reversible manner.<sup>1</sup> Recent advances in MR-guided focused ultrasound (MRgFUS) suggest that this modality could meet this challenge and enable clinically translatable neuromodulation.<sup>2–7</sup> However, the mechanism by which focused ultrasound (FUS) may directly induce changes in neural activity is unknown and is a matter of debate.<sup>6</sup> Additionally, different studies describe divergent effects of FUS on neural activity with some describing net stimulatory effects<sup>3</sup> and others describing net inhibitory effects.<sup>2,5</sup> Despite the excellent robustness and reliability of focused ultrasound techniques it is unclear how FUS alone impacts neural activity.

We propose an alternate strategy for FUS-mediated neuromodulation via FUS-gated drug delivery to the brain. This

would combine the predictability of the FUS-induced pressure field with the robustness of pharmacology. Recent application of FUS for central nervous system (CNS) drug delivery has enabled advances in the local delivery of nanoparticle-based therapeutics for varied applications including glioma treatment,<sup>8</sup> neurological disorders,<sup>9</sup> and neuroregeneration.<sup>10</sup> Although promising, all of these prior nanoparticle-based strategies depend on the transient physical opening of the blood-brain barrier (BBB) via ultrasound-induced cavitation of microbubbles. Additionally, a recent set of studies has tried to enable robust pharmacological neuromodulation via FUS-

**Received:** August 21, 2016

**Revised:** January 5, 2017

**Published:** January 17, 2017

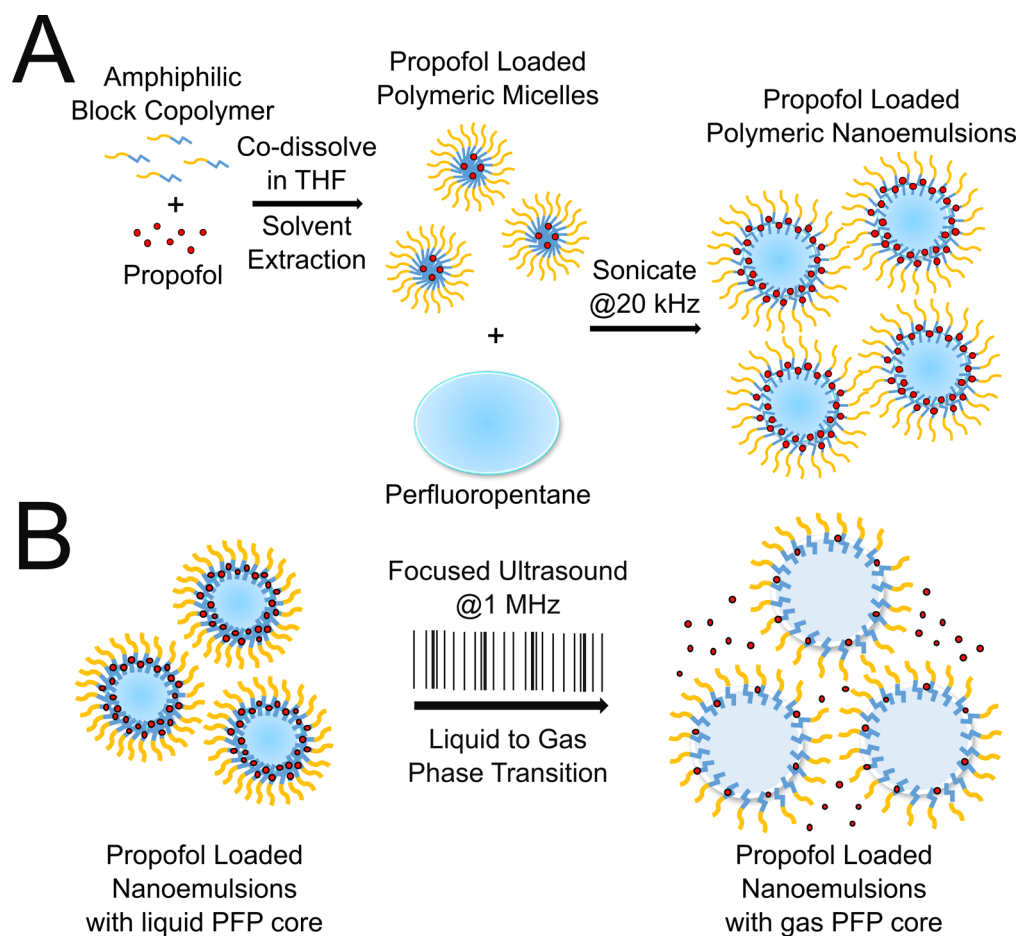


**Figure 1.** Schematic of focused ultrasound-gated drug delivery nanoparticles' preparation and use. (A) To produce the propofol-loaded nanoemulsions, first the block copolymer (yellow and blue lines) and drug (red circles) are dissolved into THF, which is followed by a solvent extraction into PBS to produce propofol-loaded polymeric micelles. These micelles then emulsify liquid perfluoropentane (PFP; light blue) through sonication at 20 kHz. (B) In use, the propofol-loaded nanoemulsions with a liquid PFP core are sonicated at a higher frequency such as 1 MHz in these experiments. That sonication induces a liquid to gas phase transition of the PFP which thins the encoated drug-loaded polymer shell, inducing drug release.

mediated BBB opening.<sup>7</sup> The BBB is a crucial component of the CNS as it maintains the optimal microenvironment for neuronal activity and protects the neurons from many endogenous and exogenous neurotoxins that are commonly found in circulation.<sup>11,12</sup>

We therefore focus on delivery of agents that may readily cross the blood-brain barrier and propose to use focused ultrasound-mediated drug uncaging from nanoparticle carriers with the ultrasound focusing providing a limit on the spatial extent of the drug-based neuromodulation. We then rely upon metabolism and redistribution of the drug to limit the temporal extent of this activity. While this limits us to small molecule lipophilic agents that are known to cross the blood brain barrier passively without the need for disruption,<sup>13</sup> many if not most drugs of neurological and psychiatric interest fall under this umbrella. In practice, after an intravenous infusion of the nanoparticles inertly labels the blood pool of the subject, FUS application releases the drug in the vascular bed of the tissue of interest in a region that is spatially limited by the size of the ultrasound focus. The drug would then cross the intact blood-brain barrier and act upon the brain parenchyma during a first-pass of perfusion. Given the availability of FDA-approved clinical MRgFUS systems that allow noninvasive transcranial focal sonication of millimeter-sized regions of the brain,<sup>14,15</sup> this

strategy could potentially allow focal, noninvasive, and safe neuromodulation with an immediate path toward clinical translation.

We have generated ultrasound-gated nanoparticle carriers of the small molecule anesthetic propofol. These particles are modified forms of prior described ultrasound-gated "phase-change" particles that were originally designed for chemotherapeutic delivery.<sup>16</sup> These particles are made of a biodegradable, biocompatible polyethylene glycol-*b*-polycaprolactone block copolymer matrix encapsulating a liquid perfluorocarbon core and the drug of interest. Under sonication, the perfluorocarbon core undergoes a liquid to gas phase transition, thereby releasing the drug cargo (Figure 1). Perfluoropentane was chosen for the perfluorocarbon core given its relatively high boiling point while encapsulated that would prevent spontaneous phase change.<sup>17</sup> This amphiphilic polyester block copolymer was chosen for the emulsifying agent as polymer perfluorocarbon nanoemulsions have been demonstrated to be more stable in general than analogous lipid nanoemulsions.<sup>18</sup> We have established the efficacy of drug release from these particles in vitro (Figure 2), as well as the in vivo biodistribution and clearance kinetics of the nanoparticles (Figure 3). As a proof-of-principle, we have further demonstrated the potency of the nanoparticles to modulate

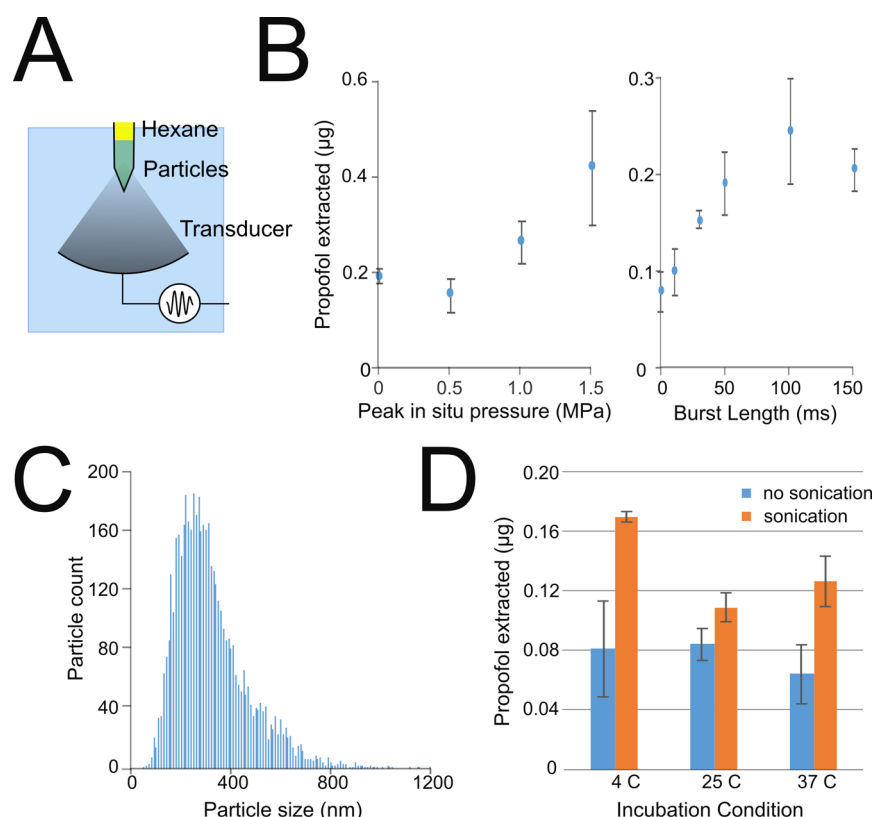


**Figure 2.** Schematic and in vitro characterization of nanoparticles enabling ultrasound-gated release of propofol for targeted neuromodulation. (A) Schematic of in vitro testing apparatus. A PCR tube containing the aqueous particle sample (green) was held at the focal spot of the FUS transducer. A layer of hexane was applied on top of the sample (yellow) to serve as a chemical sink for the released propofol. (B) Sonication induces release of propofol from particles into the medium with a dose response after a threshold peak in situ pressure of 0.5 MPa (left) and after a threshold burst length of 10 ms (right). The response to burst length saturates at 50–100 ms.  $N = 3$ –4 samples/group. (C) Histogram of particle sizes assessed by direct particle tracking demonstrates a single nanoscale peak centered at  $317.6 \pm 148.2$  nm (mean  $\pm$  SD). (D) After 2 h of incubation, particles were tested for release with 1.5 MPa peak in situ pressure and 50 ms burst lengths ( $N = 4$  samples/group). There was intact release ability after incubation, although release efficacy is relatively reduced at room (25 °C) and in vivo (37 °C) temperatures.

neural activity in vivo by using them to inducibly silence seizure activity in an acute rat seizure model (Figures 4). We have then demonstrated the safety of this technique by observing no appreciable injury nor BBB opening within the sonicated brain (Figure 5). As the components of these particles have been regarded as safe when utilized in other clinical applications,<sup>19</sup> these particles may be able to be readily combined with existent clinical transcranial MRgFUS systems<sup>14,15</sup> to enable clinical translation. Overall, this strategy provides a neuromodulation approach that has an immediate pathway to clinical translation, has a well-defined mechanism of action via the drug being delivered, does not rely upon invasive neurosurgery, gene therapy, or a deleterious action upon the brain, and is generalizable for neuromodulation via any drug that these particles could encapsulate. Indeed, this approach provides a pathway for clinical neuromodulation that is noninvasive, image-guided, and targeted to spatially compact regions of the brain with the patient otherwise able to participate in a neuropsychological assessment.

Particles that encapsulated propofol with a liquid perfluorocarbon core and a biodegradable, biocompatible polymer coating were produced (Figure 1) and sized via nanoparticle tracking analysis (Figure 2C). There was a single nanoscale peak of  $320 \pm 150$  nm (mean  $\pm$  SD). Encapsulation efficiency of the propofol was  $11.8\% \pm 1.2\%$  (mean  $\pm$  SD) yielding an encapsulated  $177 \mu\text{g} \pm 19 \mu\text{g}$  propofol per mL of particles. In

vitro particle release efficacy was assessed by focused ultrasound applied at 1 MHz center frequency in short continuous bursts with 0.5 Hz burst frequency for a total of 2 min with varying peak in situ pressure and the individual burst length, that is, the short amount of time that sonication is applied continuously. The amount of released propofol was assessed by extraction into a hexane sink (Figure 2A) and quantified via UV fluorescence. There was a dose response evident for propofol release with peak in situ pressures past a threshold of 0.5 MPa. For burst length, a release threshold of 10 ms was present with saturation of a dose response between 50 and 100 ms (Figure 2B). Particles kept in storage and in vivo-like conditions for 2 h followed by sonication at room temperature showed intact release ability, although release efficacy was reduced after 2 h of incubation at room and in vivo temperatures (Figure 2D) possibly due to diffusion of the perfluoropentane (PFP) from the core of the particles with higher temperature incubation.

To evaluate the in vivo biodistribution and intravascular residence time of the nanoparticles, the particles were initially doped with a custom synthesized hydrophobic dye. Following intravenous administration of these doped nanoparticles, timed blood samples demonstrated that the whole-blood fluorescence has a decay profile that is faithfully characterized with a double exponential decay model (Figure 3A). The initial phase decay half-life was 8.8 min and the second phase decay half-life was 270 min. Notably, the whole blood samples were expected to

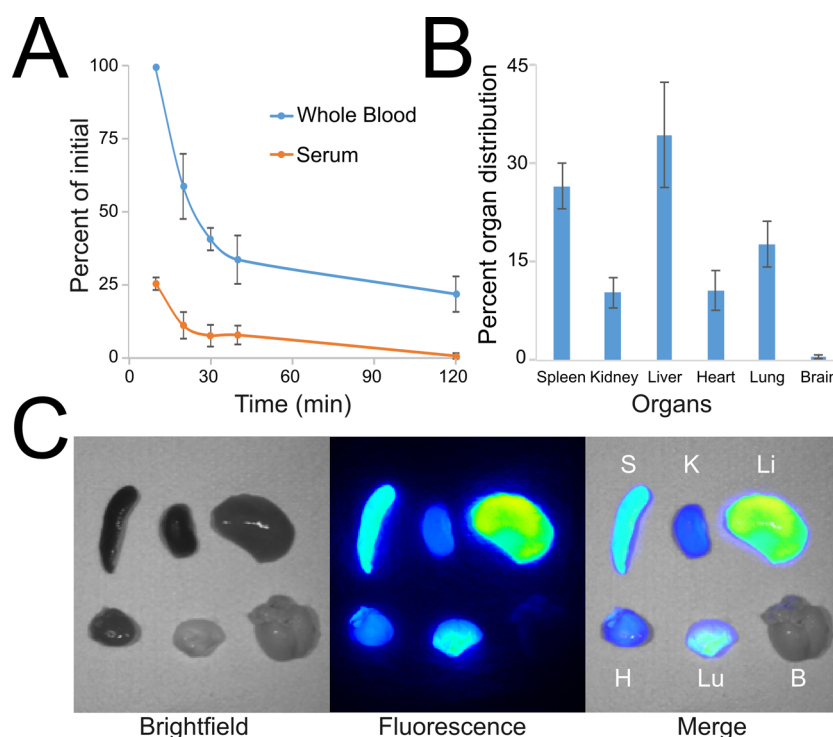


**Figure 3.** Biodistribution and clearance in vivo of the propofol-loaded nanoparticles. (A) Time course of the amount of an initial bolus of particles found in the intravascular space, as assessed by fluorescence of timed whole-blood samples after administration of propofol-loaded particles doped with an infrared fluorescent dye, compared to assessment of the serum fluorescence to determine the unbound dye kinetics. Presented are mean  $\pm$  SD, normalized by the initial whole-blood sample fluorescence ( $N = 4$  rats). (B) Organ distribution of particle uptake at 24 h (mean  $\pm$  SD for 4 rats) show that particles are sequestered in expected organs such as liver, spleen, and lung with minimal amounts seen in kidney and heart that may represent blood pool activity. No significant uptake is seen in the brain. Values are presented as their percentage of the total fluorescence across the harvested organs. (C) Sample bright field (left), fluorescence (middle), and bright field/fluorescence merged (right) images for the spleen (S), kidney (K), liver (Li), heart (H), lung (Lu), and brain (B) after harvest from a single rat.

contain both intact particles and free and micelle-bound portions of the dye. In contrast, the serum of these samples would contain free dye or potentially PEG–PCL micelle-bound dye after high-speed centrifugation pellets the cellular and nanoparticle constituents. The serum fractions showed a markedly lower fluorescence that cleared more rapidly than the whole-blood fluorescence signal, with no appreciable serum fluorescence by 2 h. The serum sample fluorescence decayed with a monoexponential profile with a half-life calculated as 8 min, notably similar to the short half-life component of the whole blood samples. After 24 h from particle administration, there was no remnant intravascular signal above background. End organ fluorescence demonstrated no evidence of non-specific particle binding to the brain (Figure 3B,C). Instead, the nanoparticles were principally taken up by the liver, spleen, and to a lesser extent the lungs, with minimal amounts in the kidney and heart.

To demonstrate and assess the functional potency of particle release in vivo, an acute pentylentetrazol (PTZ)-induced status epilepticus protocol<sup>20</sup> was developed for adult male Fischer 344 rats (Figure 4A,B). We specifically chose this protocol and preparation as prior groups have used this system to assess the degree to which FUS may directly modulate neural activity.<sup>21</sup> Following seizure induction and particle administration, there was no significant difference in baseline EEG power between animals receiving propofol-loaded particles and particles generated with no drug (“Blank”; see Supporting Information). Importantly, following FUS administration first at 1.0 MPa estimated peak in situ pressure and then at 1.5 MPa,

immediate statistically significant declines of total and theta band EEG power were seen in the animals receiving propofol-loaded particles, but not in the animals receiving blank particles (Figure 4C–F).

Ex vivo 17.6 T MRI, in vivo 11.7 T MRI, and histology confirmed that no deleterious effect of FUS and particle administration was visible (Figure 5). In particular, given the high susceptibility dependence of the MRI protocol used here (note the blooming artifact from microscopic air bubbles along the brain periphery in Figure 5A), the lack of any noted susceptibility artifact or brain parenchymal signal change within the sonicated region confirms the lack of petechial hemorrhage or other cavitation induced damage to the brain parenchyma. Notably, the 17.6 T MRI evaluation covered the entire brain in both axial and coronal planes, without interslice gaps, ensuring that a complete evaluation of the parenchyma was completed for each brain. All MRI images were reviewed by a board-certified neuroradiologist. In vivo MRI also confirmed no damage to the brain parenchyma of particle administration and sonication, and no evidence of blood-brain barrier opening with this technique (Figure 5B). Whole-brain histological sections and more focused evaluation of the sonicated dorsal dentate gyrus in comparison with the nonsonicated ventral dentate gyrus showed no evidence of parenchymal damage and certainly no damage that could be attributed to sonication (Figure 5C).

We have therefore described nanoparticles that allow focused ultrasound-induced uncaging of the small molecule anesthetic agent propofol (Figure 1) and demonstrated the in vitro and in



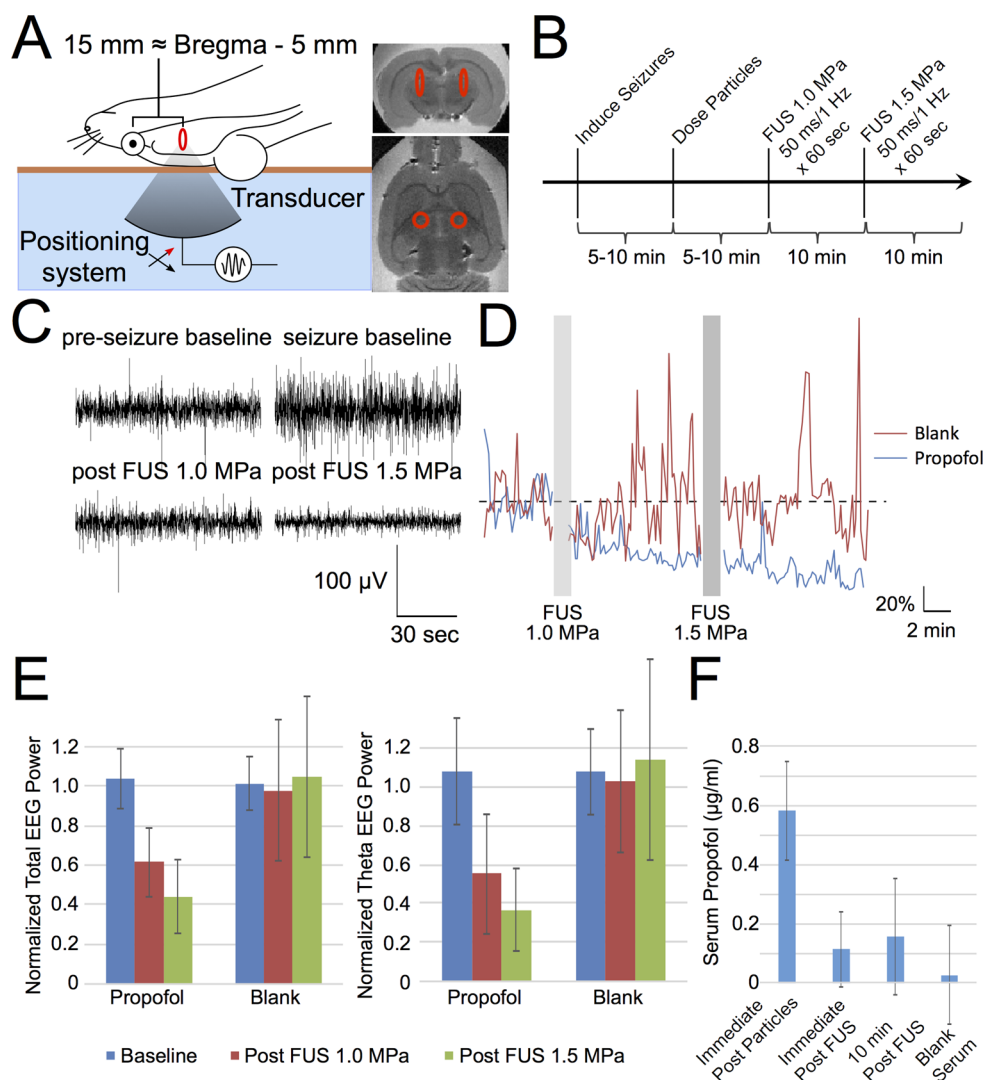


**Figure 4.** Focused ultrasound-gated propofol release is potent enough to silence seizure activity. (A) Schematic of rat positioning for this demonstration of in vivo efficacy. After removal of the dorsal scalp fur, rats were placed supine on the bed of a focused ultrasound transducer, coupled to the transducer via degassed water (light blue), a Kapton membrane filled with degassed water (orange-brown), and ultrasound gel (not pictured). Rats underwent seizure induction using the chemoconvulsant PTZ. A sonication focus (red ellipse) was developed at one target within each hemisphere, 2.5 mm lateral to midline, and 15 mm caudal to the eye center, which equals  $\sim$ 5 mm caudal to bregma. Expected location of the two sonication foci are overlaid onto ex vivo MRI images with the red ellipse indicating the fwhm of the sonication focus. (B) Schematic of experiment timing for seizure induction, particle administration, and FUS application. (C) Sample traces of EEG voltage from one rat receiving propofol-loaded particles before and after seizure-induction and focused ultrasound application at the indicated pressures. (D) Total EEG power normalized by baseline averaged across rats receiving particles loaded with either propofol (blue) or no drug (blank, red) across experiment time ( $N = 7$  propofol, 5 blank). Gray bars indicate time of FUS application at the indicated estimated in situ peak pressures in 50 ms bursts applied every 1 s for 60 s. An electrical artifact precluded EEG analysis during FUS applications. (E) Mean  $\pm$  SD of normalized total (left) and theta band (right) EEG power in the indicated time period across rats receiving propofol-loaded particles or blank particles ( $N = 7$  propofol, 5 blank). Two-way ANOVA across animals receiving both FUS treatments demonstrates significant differences with FUS application ( $p < 0.01$ ) and with particle content ( $p < 0.05$ ). Posthoc multiple comparison corrected tests show significant ( $p < 0.01$ ) differences of EEG power between baseline and each of the post FUS application periods for the propofol particle treated rats only. (F) Mean  $\pm$  SD of the HPLC-quantified serum propofol concentration of samples from  $N = 4$  rats taken immediately after propofol-loaded particle administration, immediately after sonication, and 10 min post sonication, compared to a blank serum sample. There was no appreciable serum propofol peak for the post sonication samples.

vivo efficacy of the nanoparticles as a proof-of-principle. Given that these particles have a hydrodynamic diameter of approximately 320 nm and that similar perfluorocarbon-based phase-change particles have been shown to increase diameter up to 5–6 times during sonication,<sup>16,22</sup> the maximal diameter of these particles after activation would be  $< 2 \mu\text{m}$ , suggesting no substantial risk of embolization of capillaries with these nanoparticles and their use. These particles release their drug cargo with dose responses with both peak in situ pressure and

with sonication burst length (Figure 2). The threshold peak in situ pressure of 0.5 MPa and the maximal pressure of 1.5 MPa that were used here are both achievable by current clinical transcranial MRgFUS systems.<sup>14,15</sup> Additionally, the dynamic range of the burst length dose response between 10 ms and 50–100 ms is also achievable with these clinical transcranial MRgFUS systems. These burst lengths and duty cycles are unlikely to induce substantial heating of the brain parenchyma, especially given heat dissipation by cerebral perfusion.

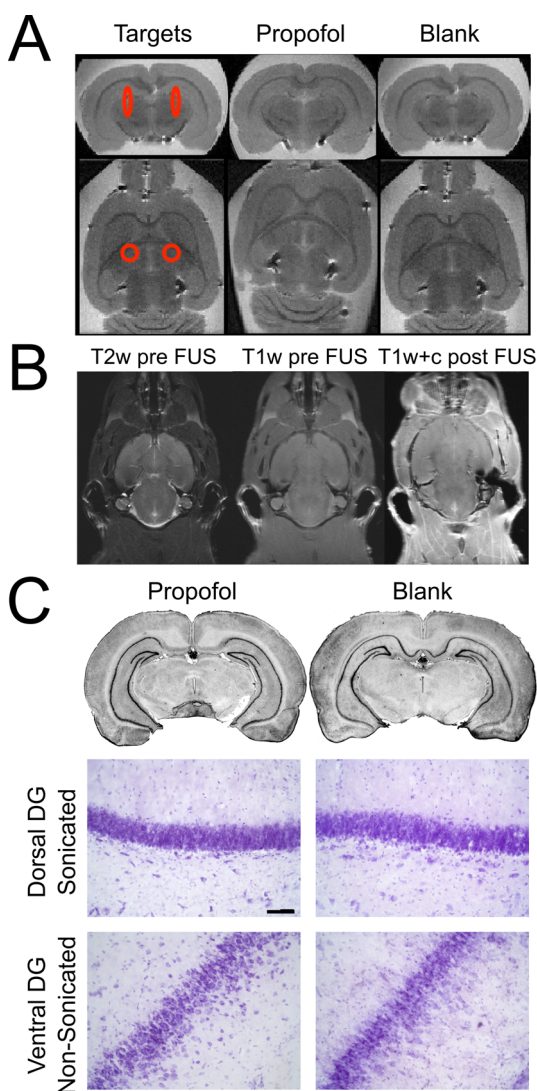


**Figure 5.** MRI and histological evaluation of brains following focused-ultrasound gated propofol release. (A) Sample whole-brain ex vivo 17.6 T MRI of rats treated with either propofol-loaded particles or blank particles and that underwent the seizure model and FUS application of Figure 4. Red ellipses in the left images indicate the expected location and fwhm of the sonication foci, overlaid onto the "Blank" images. Black spots at the periphery of the brain on the MRI images are microscopic air bubbles that show a susceptibility related blooming artifact. Notably no such findings are present near the expected sonication field to indicate tissue damage due to either particle administration or sonication. (B) The 11.7 T in vivo MRI images taken presonation (T2 and T1 weighted images left and center) and postparticle administration, postsonication, and post-contrast administration (right) show no evidence of parenchymal damage or blood-brain barrier opening due to particle administration and sonication. (C) Cresyl violet histology shows no evidence of parenchymal damage on either wide-field views (top, 4X) or magnified views (bottom, scale bar 40  $\mu\text{m}$ ) for either propofol-loaded or blank particle-treated animals that received the full sonication protocol of Figure 4. The more medial dorsal dentate gyrus (DG) was within the sonication trajectory. The more lateral ventral dentate gyrus was not within the sonication trajectory and serves as a negative control for assessment of damage.

We were able to use particles doped with an IR fluorescent dye as a surrogate marker of particle intravascular residence and distribution (Figure 3). The serum fluorescence, which would

contain the unbound free dye fraction, showed a much more rapid clearance from the blood pool than the whole-blood samples that represent both the particle-bound and unbound fractions. The whole-blood fluorescence particle elimination profile showed two phases: an initial rapid (9 min half-life) phase that likely corresponds to the unbound dye fraction of the sample, and a slower (270 min half-life) phase that more represents the particle decay profile itself (Figure 3A). This half-life would allow enough time for a clinically relevant intervention with these particles, but not so long of a particle vascular residence time that it would preclude repeat particle administration or would suggest a potential toxicity of extended particle residence in the body. The lack of particle uptake in the brain (Figure 3B,C) confirms that our results are unlikely to be due to particle crossing of the blood brain barrier, particle binding to the brain, or some other nonspecific action of the particles upon the brain. The finding that the liver and spleen primarily take up these particles is expected as the reticuloendothelial system generally sequesters nanoscale material.<sup>23</sup>

The ability of focused ultrasound to activate the intravascular propofol-loaded particles and yield silencing of seizure activity in vivo (Figure 4) indicates that these particles indeed can enable a potent neuromodulatory effect upon focused ultrasound application. Crucially, given that there was no significant effect of sonication in rats receiving the blank particles and seeing as the blank particles were otherwise constructed exactly the same as the propofol-loaded particles, the effects seen here are specifically related to the release of propofol in this system and not a nonspecific effect of ultrasound or particle interaction with neural tissue or of the individual polymer or perfluorocarbon particle constituents. Given that our total encapsulation efficiency of 177  $\mu\text{g}/\text{mL}$  translates to  $\sim 1$  mg/kg in these experiments and that a normal loading dose for anesthetic effect in rats is an order of magnitude higher at 10 mg/kg,<sup>24</sup> it is unlikely that our results are due to a nonspecific leak of the propofol from the particles. Indeed, serum propofol concentrations taken immediately and 10 min after sonication showed no appreciable propofol above the background (Figure 4F), indicating that this propofol release was likely limited to the brain, without nonspecific systemic delivery. The detectable serum propofol seen immediately following particle administration likely reflects a small amount of free propofol in the particle batch given our method of production, although this level of  $\sim 0.6$   $\mu\text{g}/\text{mL}$  is an order of magnitude less than the typical serum concentrations of propofol thought to be necessary for an anesthetic effect. Taken together, these results suggest that these particles indeed yield a higher local drug concentration in the brain following FUS application than might be suggested by the raw total amount of drug delivered in the bolus intravenous dose. Additionally, given the fast 2–3 min distribution half-life of propofol from the blood-pool,<sup>25</sup> given that we waited 5–10 min from particle administration to FUS application, and given that we did not see significant differences in the baseline EEG power between propofol and blank treated rats, it is unlikely that free or loosely bound propofol in the particle solution could have substantially contributed to our results. Notably, the EEG power was seen to decrease immediately following FUS application suggesting that the kinetics of this neuromodulatory effect are rapid (Figure 4D). Additionally, we did not observe any deleterious consequence to the brains with ex vivo MRI, in vivo MRI, or post hoc histology (Figure 5), suggesting that these effects are

not due to a nonspecific damage of the brain parenchyma. Indeed, the lack of blood-brain barrier opening with this technique (Figure 5B) confirms the safety of this technique and the distinction of this technique between it and other proposed methods of FUS-mediated neuromodulation.<sup>7,21</sup>

In this study, we have not directly visualized the particle activation in vivo to assess the effective spatial resolution of this technique. Additionally, the volume conduction effect of EEG signals, particularly for subdermal EEG, and the nature of the generalized status epilepticus model used for this study limits our ability to spatially resolve this signal in this in vivo preparation. Similarly, given the acute nature of PTZ-induced seizures that may not recur substantially once they are aborted, this study protocol is limited in ability to determine over what time interval the action of the gated propofol persists. Those limitations said, the in situ ultrasound focus induced by the particular ultrasound transducer used in this study is known to have a fwhm of  $\sim 1.5$  mm transaxially and  $\sim 5$  mm longitudinally at 1 MHz (personal communication with the vendor, FUS Instruments, Toronto, CA), providing an effective initial spatial extent for the action of the particles in this preparation. Additionally, we saw no substantial systemic propofol load with sonication (Figure 4F), confirming that the propofol release was likely limited to the brain. While groups have shown that activated perfluorocarbon particles may induce further activation of unsonicated particles in static solutions,<sup>16</sup> we would expect cerebral perfusion to rapidly clear the activated particles from the sonication field, especially given the lack of particle binding to the brain (Figure 3), thereby limiting this potential confound. Additionally, the temporal residence of propofol in the brain and its time of action is known to be rapid on the order of minutes or even tens of seconds<sup>26</sup> and similar to the time-scales used in this experiment. This time of action would be clinically practical for neuropsychological assessment, as evidenced by the current protocol of the Wada test,<sup>27</sup> which is used for clinical mapping of the laterality of brain functions. Given the size of the rat cerebrum ( $\sim 15 \times 15 \times 10$  mm<sup>28</sup>) and the technical limitations of signal volume conduction in subdermal EEG, further characterization of the spatial and temporal resolution of this technique will necessitate experiments that assess baseline nonseizure neural activity, likely in larger animal models, and potentially with a different measure of neural activity, such as fMRI or PET. Nonetheless, our results provide a proof-of-principle that these nanoparticles yield potent inducible neuromodulation using noninvasive focused ultrasound and that this approach has the potential to enable precise spatial (mm) and temporal (min) control of brain activity, with a pathway to clinical translation.

With regard to clinical translation, each component of these particles has been previously approved for clinical use in different contexts.<sup>19</sup> Additionally, the sonication pressures and burst lengths used in this study are well achievable by FDA-approved transcranial MRgFUS systems that are currently in clinical use.<sup>14</sup> Taken together, this provides a pathway toward clinical translation that is otherwise unavailable to other targeted molecular neuromodulation strategies. Further, the chemistry that enables these particles to encapsulate a given drug relies mainly upon the lipophilicity of the drug in question, so that it may bind the hydrophobic domains of the encapsulating block copolymer and the hydrophobic polymer–perfluorocarbon interface. Given that most molecules that passively cross the blood-brain barrier are highly lipophilic, this suggests that the nanotechnology strategy presented here could

be adapted for focal and targeted delivery of most any small molecule that naturally crosses the blood-brain barrier, including imaging agents as well as compounds that act directly upon the adrenergic, serotonergic, or dopaminergic systems, in addition to the excitation/inhibition axis that propofol modulates. This opens the door to a wide variety of potential nanotechnological tools for targeted clinical modulation of brain activity.

## ■ ASSOCIATED CONTENT

### § Supporting Information

The Supporting Information is available free of charge on the ACS Publications website at DOI: 10.1021/acs.nanolett.6b03517.

Supplementary methods including nanoemulsion formulation, in vivo biodistribution methods, in vivo efficacy methods, and MRI/histology methods (PDF)

## ■ AUTHOR INFORMATION

### Corresponding Authors

\*E-mail: (R.D.A.) [rairan@stanford.edu](mailto:rairan@stanford.edu).

\*E-mail: (J.J.G.) [green@jhu.edu](mailto:green@jhu.edu).

### ORCID

Raag D. Airan: 0000-0001-5259-5606

Martin G. Pomper: 0000-0001-6753-3010

Shilpa D. Kadam: 0000-0001-5136-9594

Jordan J. Green: 0000-0003-4176-3808

### Author Contributions

Overall design of the experiments (R.D.A., R.A.M., N.P.K.E., K.F., M.G.P., S.D.K., J.J.G.); nanoparticle generation and characterization (R.D.A., R.A.M., J.J.G.); focused ultrasound system modification and use (R.D.A., R.A.M., N.P.K.E., K.F.); seizure model development, EEG acquisition and analysis, and histology (R.D.A., S.D.K.); ex vivo and in vivo MRI (R.D.A., N.P.K.E.); HPLC serum analysis (R.A.M., K.R.R., J.J.G.). The manuscript was written through contributions of all authors. All authors have given approval to the final version of the manuscript. R.D.A. and R.A.M. contributed equally.

### Funding

This work was funded via grant support from the NIH (NIBIB R01EB016721 and R01EB022148, J.J.G.; NICHD R21HD073105, S.D.K.; NCI P50CA058236, M.G.P.; NCI F31CA214147, R.A.M.), Philips Inc., the Foundation of the American Society for Neuroradiology, and the Walter and Mary Ciceric Foundation. R.A.M. thanks that Achievement Rewards for College Scientists Metro-DC Chapter for fellowship support. K.R.R. thanks the National Science Foundation Graduate Research Fellowship Program (DGE-1232825) for fellowship support.

### Notes

The authors declare the following competing financial interest(s): Dr. Nicholas Ellen has worked in the past as a paid consultant for FUS Instruments, Inc.

## ■ ACKNOWLEDGMENTS

We are incredibly indebted to Dr. Jonathan Lewin (Emory) for the advice, support, and mentorship he provided during the planning and execution of this work. Dr. Andrew Neice (OHSU) and Dr. Michael P. Bokoch (UCSF) provided critical discussions during the exploratory phase of this work. We greatly appreciate the helpful assistance of Qiuyin Ren, Callie



Deng, David Wilson, and Brandon Carter (JHU) in the completion of these experiments. We additionally appreciate the thorough reviews and critical comments provided by the reviewers.

## ■ ABBREVIATIONS

FUS, focused ultrasound; BBB, blood-brain barrier; CNS, central nervous system; MRgFUS, magnetic resonance guided focused ultrasound; EEG, electroencephalography; MRI, magnetic resonance imaging; fwhm, full width at half-maximum; PFP, perfluoropentane; PTZ, pentylenetetrazol

## ■ REFERENCES

- (1) Jorgenson, L. A.; et al. *Philos. Trans. R. Soc. London B. Biol. Sci.* **2015**, 370, 214–222.
- (2) Kim, H.; Park, M. Y.; Lee, S. D.; Lee, W.; Chiu, A.; Yoo, S.-S. *NeuroReport* **2015**, 26, 211–215.
- (3) King, R. L.; Brown, J. R.; Newsome, W. T.; Pauly, K. B. *Ultrasound Med. Biol.* **2013**, 39, 312–331.
- (4) King, R. L.; Brown, J. R.; Pauly, K. B. *Ultrasound Med. Biol.* **2014**, 40, 1512–1522.
- (5) Legon, W.; Sato, T. F.; Opitz, A.; Mueller, J.; Barbour, A.; Williams, A.; Tyler, W. J. *Nat. Neurosci.* **2014**, 17, 322–329.
- (6) Sassaroli, E.; Vykhodtseva, N. J. *Ther. Ultrasound* **2016**, 4, 17.
- (7) McDannold, N.; Zhang, Y.; Power, C.; Arvanitis, C. D.; Vykhodtseva, N.; Livingstone, M. *Sci. Rep.* **2015**, 5, 16253.
- (8) Oberoi, R. K.; Parrish, K. E.; Sio, T. T.; Mittapalli, R. K.; Elmquist, W. F.; Sarkaria, J. N. *Neuro. Oncol.* **2016**, 18, 27–36.
- (9) Lin, C. Y.; Hsieh, H. Y.; Chen, C. M.; Wu, S. R.; Tsai, C. H.; Huang, C. Y.; Hua, M. Y.; Wei, K. C.; Yeh, C. K.; Liu, H. L. *J. Controlled Release* **2016**, 235, 72–81.
- (10) Samiotaki, G.; Acosta, C.; Wang, S.; Konofagou, E. E. *J. Cereb. Blood Flow Metab.* **2015**, 35, 611–622.
- (11) Abbott, N. J.; Patabendige, A. A. K.; Dolman, D. E. M.; Yusof, S. R.; Begley, D. J. *Neurobiol. Dis.* **2010**, 37, 13–25.
- (12) Persidsky, Y.; Ramirez, S. H.; Haorah, J.; Kanmogne, G. D. *J. Neuroimmune Pharmacol.* **2006**, 1, 223–236.
- (13) Sharma, G.; Lakkadwala, S.; Modgil, A.; Singh, J. *Int. J. Mol. Sci.* **2016**, 17, 806.
- (14) Ghanouni, P.; Pauly, K. B.; Elias, W. J.; Henderson, J.; Sheehan, J.; Monteith, S.; Wintermark, M. *AJR, Am. J. Roentgenol.* **2015**, 205, 150–159.
- (15) McDannold, N.; Clement, G. T.; Black, P.; Jolesz, F.; Hynynen, K. *Neurosurgery* **2010**, 66, 323–332.
- (16) Rapoport, N. *Wiley Interdiscip. Rev. Nanomed. Nanobiotechnol.* **2012**, 4, 492–510.
- (17) Sheeran, P. S.; Dayton, P. A. *Curr. Pharm. Des.* **2012**, 18, 2152–2165.
- (18) Rapoport, N. *Adv. Exp. Med. Biol.* **2016**, 880, 221–241.
- (19) Kamaly, N.; Xiao, Z.; Valencia, P. M.; Radovic-Moreno, A. F.; Farokhzad, O. C. *Chem. Soc. Rev.* **2012**, 41, 2971.
- (20) Lüttjohann, A.; Fabene, P. F.; van Luijckelaar, G. *Physiol. Behav.* **2009**, 98, 579–586.
- (21) Min, B. K.; Bystritsky, A.; Jung, K. I.; Fischer, K.; Zhang, Y.; Maeng, L. S.; Park, S. I.; Chung, Y. A.; Jolesz, F. A.; Yoo, S. S. *BMC Neurosci.* **2011**, 12, 23.
- (22) Gao, Z.; Kennedy, A. M.; Christensen, D. A.; Rapoport, N. Y. *Ultrasonics* **2008**, 48, 260–270.
- (23) Sadauskas, E.; Wallin, H.; Stoltenberg, M.; Vogel, U.; Doering, P.; Larsen, A.; Danscher, G. *Part. Fibre Toxicol.* **2007**, 4, 10.
- (24) Gaertner, D. J.; Hallman, T. M.; Hankenson, F. C.; Batchelder, M. A. *Anesthesia and Analgesia in Laboratory Animals* **2008**, 239–297.
- (25) Kanto, J.; Gepts, E. *Clin. Pharmacokinet.* **1989**, 17, 308–326.
- (26) Upton, R. N.; Ludbrook, G. L. *Br. J. Anaesth.* **1997**, 79, 497–504.
- (27) Baxendale, S. *Curr. Opin. Neurol.* **2009**, 22, 185–189.
- (28) Paxinos, G.; Watson, C. *The rat brain in stereotaxic coordinates*; Elsevier: San Diego, CA, 2007; pp 1–78.